Available online at www.sciencedirect.com
ScienceDirect
Journal of Photochemistry and Photobiology A: Chemistry 192 (2007) 188–196
Journal of Photochemistry and Photobiology A:Chemistry
www.elsevier.com/locate/jphotochem

Fluorescence properties of the derivatives of oxazolo[4,5-*b*]pyridyne

Marek Mac [a,*], Wojciech Baran [b], Tomasz Uchacz [a], Barbara Baran [c,1], Marzena Suder [c,1], Sebastian Leśniewski [a]

[a] *Faculty of Chemistry, Jagiellonian University, 30-060 Kraków, Ingardena St. 3, Poland*
[b] *Department of Chemistry, University of Agriculture, Balicka St. 122, 31-149 Kraków, Poland*
[c] *Material Sciences, Jagiellonian University, Kraków, Poland*

Received 20 December 2006; received in revised form 21 May 2007; accepted 22 May 2007
Available online 25 May 2007

Abstract

The fluorescence behaviour of a family of new dyes based on the oxazolo[4,5-*b*]pyridine ring has been investigated. It was found that introduction of electron withdrawing and electron donating groups into the oxazolo[4,5-*b*]pyridine molecule causes an increase of the ground and excited state dipole moments. The observed fluorescence has a strong charge transfer character and was investigated in terms of radiative back electron transfer theory. In water–acetonitrile solutions the compounds behave as bases forming fluorescing cations in the presence of inorganic acid. The protonation centres are different depending on the substituent. In the case of 2-(4-*N*,*N*-diethylaminophenyl)oxazolo[4,5-*b*]pyridine the protonation is complex and formation of a bication of this compound has been determined. These observations are consistent with quantum chemical calculations.

Keywords: Electron transfer; Fluorescence; Actinometric titration; Foerster cycle

1. Introduction

Oxazolo[4,5-*b*]pyridine derivatives containing different substituents have been intensively investigated recently because of their biological activity. Their activity depends usually on nature of substituents attached to the oxazolo[4,5-*b*]pyridine skeleton. For example, 2-aryloxazolo[4,5-*b*]pyridines show anti-inflamator [1], anti-pyretic [2] and analgesic properties. A paper that describes the absorption spectra of 2-diazaderivatives has been published by Viscardi et al. [3], but the fluorescence properties of these dyes have not been investigated yet. Many oxazolopyridines show fluorescence emission in the visible region of the spectrum. It makes them good candidates for construction of LED devices or nonlinear optic systems.

The aim of this work is to investigate the basic fluorescence properties of some oxazolo[4,5-*b*]pyridine derivatives with different substituents as well as their acid–base properties. The presence of strong basic and electron deficient pyridine ring makes these systems different from the better known benzoxazol derivatives.

2. Experimental

2.1. Synthesis of oxazolo[4,5-b]pyridines

The oxazolo[4,5-*b*]pyridine skeleton is usually obtained via oxazole ring closure with benzoic acid in polyphosphoric acid (PPA). The method is simple and convenient but adequately substituted 2-amino 3-hydroxypyridine derivatives are necessary. These reactants are hard to obtain commercially. In such cases the modification of the obtained compound is necessary (as in the CN derivative). The synthesis routes are presented in Fig. 1.

2.1.1. Oxazolo[4,5-b]pyridin-2(3H)-thione (*3*)

Obtained according to paper [4]. Mp: 243 °C. Lit.: 245 °C.

2.1.2. Oxazolo[4,5-b]pyridin-2(3H)-one (*4*)

Obtained according to paper [5]. Mp: 212–213 °C. Lit.: 211–212 °C.

2.1.3. 6-Bromoxazolo[4,5-b]pyridin-2(3H)-one (*5*)

Obtained according to paper [6]. Mp: 229–230 °C. Lit.: 230 °C.

* Corresponding author. Tel.: +48 12 6632262; fax: +48 12 6340515.
E-mail address: mac@chemia.uj.edu.pl (M. Mac).
[1] Students of Material Sciences of Jagiellonian University.

1010-6030/$ – see front matter © 2007 Elsevier B.V. All rights reserved.
doi:10.1016/j.jphotochem.2007.05.023

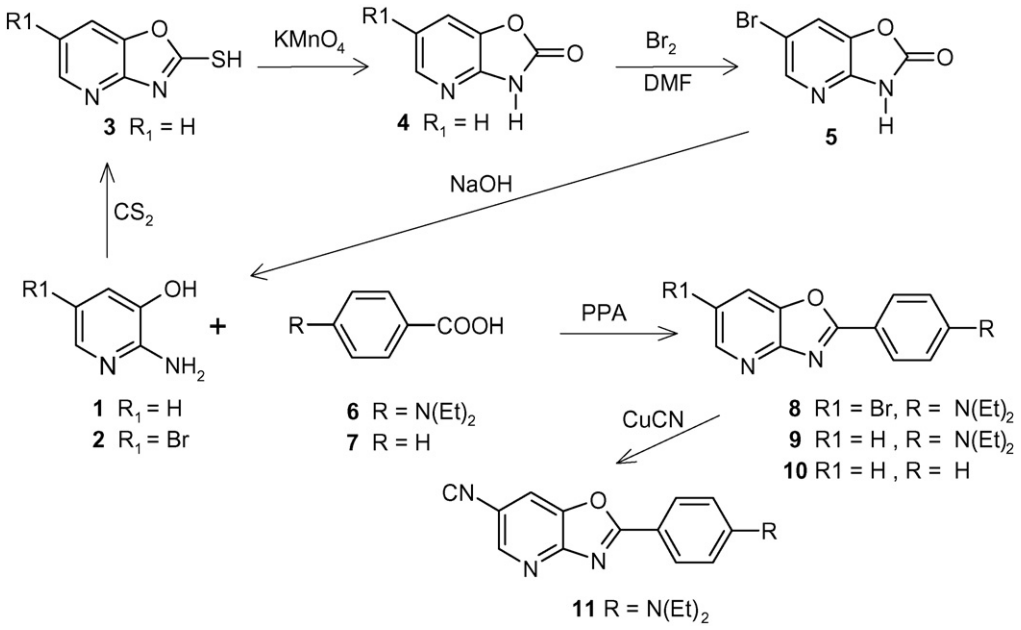

Fig. 1. Synthesis of oxazolo[4,5-*b*]pyridines.

*2.1.4. 2-Amino-5-bromo-3-hydroxypyridine (**2**)*

Obtained according to paper [6]. Mp: 205 °C. Lit.: 204–205 °C.

*2.1.5. 2-Phenyl-oxazolo[4,5-b] pyridine (**10**) (P1)*

Obtained according to paper [1]. Mp: 126 °C. Lit.: 127–127.5 °C (Fig. 2).

*2.1.6. 6-Bromo-2-(4-N,N-diethylaminophenyl)oxazolo[4,5-b]pyridine (**8**)*
(P3)

Equimolar mixture of 2-amino-5-bromo-3-hydroxypyridine (**2**) (1.89 g, 10 mM) and *N*,*N*-diethylaminobenzoic acid (**6**) (1.93 g, 10 mM) was heated in 50 g polyphosphoric acid in the temperature of 145 °C for 12 h. After cooling to room temperature the solution was poured in a mixture of ice and 50 cm^3 concentrated ammonium hydroxide. The precipitated solid was filtered off, dried, and purified by multiple crystallization from toluene–*n*-heptane mixture.

Mp: 147–148 °C. Yield 71.70% after first crystallization. HRMS: Calculated exact mass for $C_{16}H_{16}BrN_3O$: 345,0477. Found: 345,0454. ^{1}H NMR ($CDCl_3$) δ: 1205–1250 (t, 6 H, H_{ethyl}), 3412–3482 (q, 4H, H_{ethyl}), 6718–6748 (d, J = 9232 Hz, 2H, H_{arom}), 7780–7775 (d, J = 2052, 1H, H-7), 8077–8107 (d, J = 9232 Hz, 2H, H_{arom}), 8475–8515 (d, J = 2052, 1H, H-5).

*2.1.7. 2-(4-N,N-diethylaminophenyl)oxazolo[4,5-b]-pyridine (**9**) (P2)*

Equimolar mixture of 2-amino-3-hydroxypyridine (**1**) (1.10 g, 10 mM) and *N*,*N*-diethylaminobenzoic acid (**6**) (1.93 g, 10 mM) was heated in polyphosphoric acid in the temperature of 145 °C for 12 h. After cooling to room temperature the solution was poured in a mixture of ice and 50 cm^3 concentrated ammonium hydroxide. The precipitated solid was filtered off, dried, and purified by multiple crystallization from toluene–*n*-heptane mixture.

Mp: 205–207 °C. Yield 84.9% after first crystallization. HRMS: Calculated exact mass for $C_{16}H_{17}N_3O$: 267,1372. Found: 267,1318. ^{1}H NMR ($CDCl_3$) δ: 1218 (t, 6 H, H_{ethyl}), 3403–3473 (q, 4H, H_{ethyl}), 6726–6755 (d, J = 8719 Hz, 2H, H_{arom}), 7138–7181 (dd, 1H, H-6), 7719–7775 (dd, J = 9232, 1H, H-7), 8111–8141 (d, J = 9232 Hz, 2H, H_{arom}), 8475–8554 (dd, J = 6155, 1H, H-5).

*2.1.8. 6-Cyano-2-(4-N,N-diethylaminophenyl)oxazolo[4,5-b]pyridine (**11**)*
(P4)

The mixture of 1.73 g (0.005 mole) of 6-bromo-2-(4-*N*,*N*-diethylaminophenyl)oxazolo[4,5-*b*]pyridine (**8**) and 0.89 g (0.01 mole) of CuCN was heated in *N*,*N*-dimethylpyrolidon at 200 °C over night. After cooling the mixture was added to concentrated ammonium hydroxide and the resulting solid was filtered off. Several crystallization cycles from EtOH yielded yellow needle-shaped crystals.

Mp: 233–235 °C. Yield 49.5% after first crystallization. HRMS: Calculated exact mass for $C_{17}H_{16}N_4O$: 292,1324. Found: 292,143. ^{1}H NMR ($CDCl_3$) δ: 1229–1277 (t, 6 H, H_{ethyl}), 3444–3516 (q, 4H, H_{ethyl}), 6807–6836 (d, J = 8719 Hz, 2H, H_{arom}), 7945–7952 (d, J = 2052, 1H, H-7), 8146–8177 (d, J = 9232 Hz, 2H, H_{arom}), 8744–8752 (d, J = 2052, 1H, H-5).

The investigated compounds are presented below with their chemical names and the abbreviations used in text. The C^{13} NMR spectra of the novel compounds (P2–P4) are presented in Fig. 2.

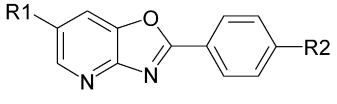

R1 = R2 = H, 2-phenyl-oxazolo[4,5-*b*] pyridine (P1);

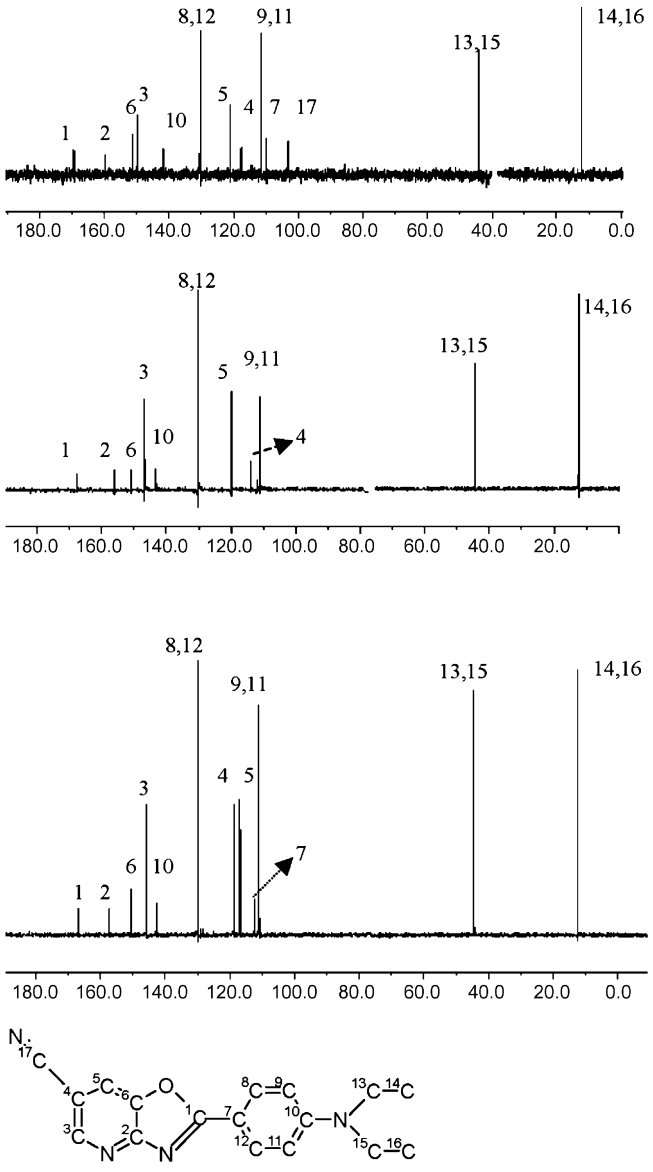

Fig. 2. C^{13} NMR spectra of P2, P3 and P4 (bottom, middle and top, respectively) in $CDCl_3$ (P2 and P3) and DMSO-d_6 (P4). The NMR signals of the solvents were removed from the spectra. NMR signals were ascribed to the carbon atoms whose positions are indicated on the structure.

R1 = H, R2 = $N(C_2H_5)_2$ 2-(4-*N*,*N*-diethylaminophenyl) oxazolo[4,5-*b*]pyridine (P2);
R1 = Br, R2 = $N(C_2H_5)_2$, 6-bromo-2-(4-*N*,*N*-diethylaminophenyl)oxazolo[4,5-*b*]pyridine (P3);
R1 = CN, R2 = $N(C_2H_5)_2$, 6-cyano-2-(4-*N*,*N*-diethylaminophenyl)oxazolo[4,5-*b*]pyridine (P4).

2.2. Fluorescence measurements (steady state and time-resolved)

The solvents: cyclohexane (CHX), dibutyl ether (DBE), ethyl acetate (EtAc), tetrahydrofuran (THF), ethyl bromide (EtBr), ethyl iodide (EtI), glycerol triacetate (GTA), dichloromethane ($MeCl_2$), acetone (ACE), aliphatic alcohols (from methanol to octanol), acetonitrile (ACN), dimethylformamide (DMF), propylene carbonate (PC) and dimethyl sulfoxide (DMSO) were of spectroscopic grade and were used as received (all from Aldrich). All of the solvents did not show any traces of fluorescence. For fluorescence and transient absorption measurements the solutions of the dyes were degassed using multiple freeze–pump–thaw cycles. The sample concentration of the dyes for spectroscopic measurements was ca. 10^{-5} M (this corresponds to absorbances of ca. 0.2–0.3 at the excitation wavelengths used in the fluorescence investigations).

Fluorescence measurements were performed on a home-built spectrofluorimeter and a time-correlated single photon counting setup. For time-resolved fluorescence measurements a picosecond diode laser ($\lambda = 400$ nm, 70 ps pulse duration) or nanosecond diode ($\lambda = 370$ nm, 1 ns pulse duration) (both from IBH-UK) were used as the excitation source. For steady-state fluorescence measurements a 313, 365 or 405-nm line of medium-pressure mercury lamp was used. The fluorescence quantum yields measurements were carried out with quinine sulphate in water ($\Phi_{fl} = 0.55$) [7] as an actinometer.

2.3. Calculations

Electron transfer parameters were recovered using the CT fluorescence band shape analysis, as described in previous papers [8]. The MINUITS procedure from the CERN Library was used to fit the experimental spectra with model band shapes.

Quantum chemical calculations were done using the GAUSSIAN 03 quantum chemistry computational package [9]. The DFT (B3LYP/6-31+G*) method was used for ground state geometry optimization of P1, P2, P3 and P4, and subsequent calculation of dipole moments and atomic charges in these molecules. The atomic charges were obtained by fitting the electrostatic potential at the Van der Waals surface, as implemented in Gaussian.

3. Results

Absorption spectra of the compounds P1, P2, P3, and P4 in acetonitrile are presented in Fig. 3.

As we can see, the introduction of the electrodonating and electroaccepting groups into oxazolo[4,5-*b*]pyridine ring causes the vibrational structure of the spectra to vanish. This vibrational structure is observed in "bare" oxazolo[4,5-*b*]pyridine in all solvents. A batochromic shift is observed in the absorption spectra in systems containing amine, Br and CN groups.

The absorption spectra of all compounds except the "bare" oxazolo[4,5-*b*]pyridine show a behaviour typical for charge transfer compounds, i.e. the position of the first absorption band shifts to lower wavenumbers when the solvent polarity increases, as it is shown for the compound P2 in Fig. 3.

Fluorescence spectra of the compounds P2–P4 exhibit a well-known solvent polarity dependence, i.e. increasing solvent polarity causes a batochromic shift of the position of the maximum of fluorescence spectra. For the compound P1, a vibrational

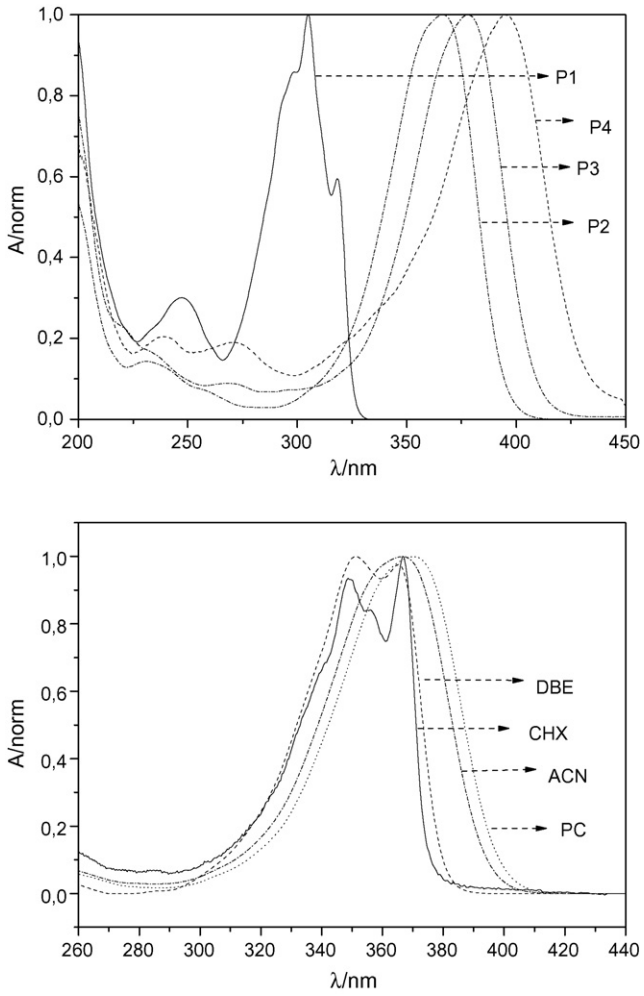

Fig. 3. Normalized absorption spectra of the compounds P1, P2, P3 and P4 in acetonitrile (top) and that of P2 in solvents of varying polarities (bottom).

structure in the fluorescence is observed, almost unchanged in all solvents—only a slight diffusion occurs when the polarity of the solvent increases. An example of the fluorescence behaviour is presented in Fig. 4.

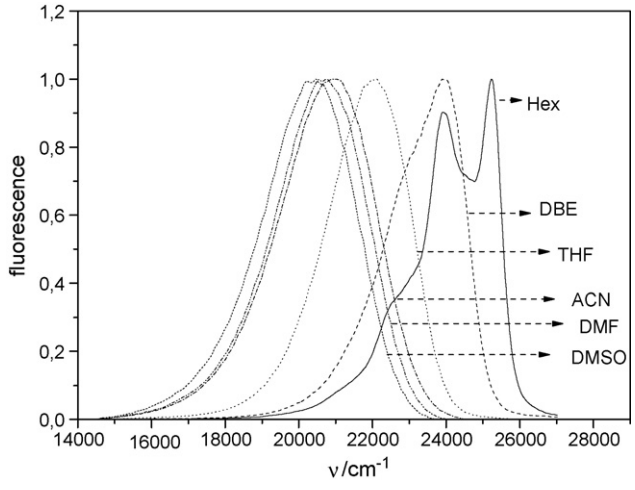

Fig. 4. Fluorescence of P4 in solvents of varying polarity (as indicated by the acronyms in the figure).

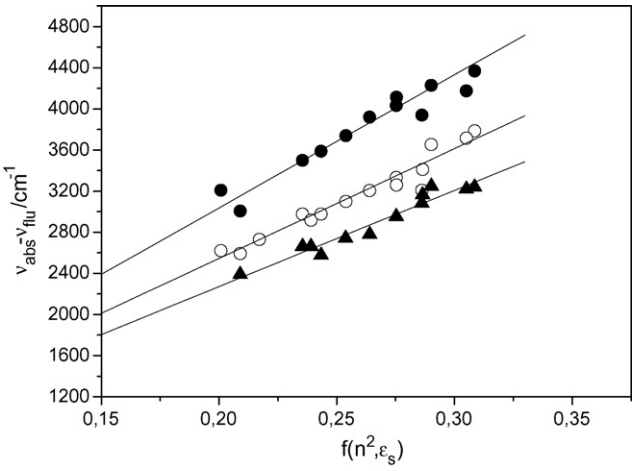

Fig. 5. Lippert–Mataga plot for the dependence of the difference between the position of the maxima of the absorption and fluorescence bands on solvent polarity function $f(\varepsilon_s, n^2) = (((\varepsilon_s - 1)/(2\varepsilon_s + 1)) - ((n^2 - 1)/(2n^2 + 1)))$ for P2 (black triangles), P3 (open circles) and P4 (black circles) (correlation coefficient $R = 0.97$ in all cases).

Dependence of the difference between the position of the maximum of the first absorption band and that of the fluorescence on solvent polarity function is given by the well-known Lippert–Mataga equation [10]. We observe a considerable batochromic shift in the position of the fluorescence maximum for molecules P3 and P4 as presented representatively for P4 in Fig. 4. This shift can be accounted for by assuming that the emitting singlet state has a dipole moment much larger than the ground state, strongly suggesting that it has an internal charge transfer character. For such a biradical-type state the dipole moment can be experimentally calculated from the Lippert–Mataga relationship, neglecting the mean solute polarizability ($\alpha \approx \alpha_e \approx \alpha_g \approx 0$) [10].

The changes of the dipole moments upon excitation estimated from the Lippert–Mataga analysis (Fig. 5) are: 10.4, 12.2, and 13.5 D for P2, P3 and P4, respectively. The estimated (in vacuo) ground state dipole moments obtained from quantum chemical calculations are 6.3, and 7.8 and 11.2 D for P2, P3 and P4, respectively. This suggest that the excitation of the molecule (P2–P4) increases the dipole moment significantly and in the excited state the dipole moments for P2, P3 and P4 have a magnitude of about 17, 20 and 25 D, respectively.

The fluorescence of these compounds can therefore be analysed in terms of the Marcus' radiative back electron transfer theory [11]. The CT fluorescence profile is described by the following formula [12] as:

$$\mathrm{CT}(\nu) = n^3\nu^3\left(\frac{n^2+2}{3}\right)^2 \frac{64\pi^2}{3h^3} M^2 \sum_{j=0}^{\infty} \frac{S^j}{j!} (4\pi\lambda_s kT)^{-1/2} \times \exp\left(-\frac{(\Delta G_{et} + jh\nu_v + \lambda_s + h\nu)^2}{4\lambda_s kT}\right), \quad (1)$$

where M is the transition dipole moment, λ_s the solvent reorganization energy and ΔG_{et} is the energy difference between the CT and ground states. S is the displacement parameter, connected

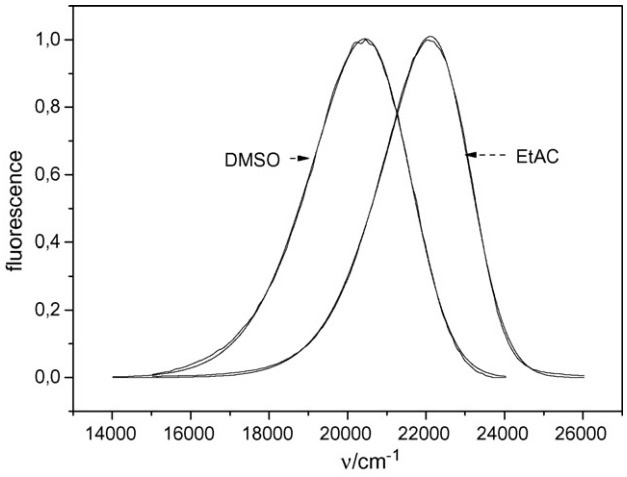

Fig. 6. Corrected and normalized CT fluorescence spectra of P4 in EtAc and DMSO and their theoretical predictions given by Eq. (1). The fitted parameters are $\Delta G_{et} = -2.98$ (-2.85) eV, $\lambda_s = 0.217$ (0.303) eV and $\lambda_{in} = 0.11$ eV for both solvents. The values in parentheses correspond to DMSO solution.

with the internal reorganization energy (λ_{in}) and aromatic ring skeletal vibration ($h\nu_v = 1600\,cm^{-1}$) by the relation:

$$S = \frac{\lambda_{in}}{h\nu_v}. \tag{1a}$$

The integer j appearing in Eq. (1) is the number of quanta of this mode.

The band-shape fitting procedure applied for theses systems in solvents of different polarity showed that the internal reorganization energy parameter (λ_{in}) does not depend on the polarity of the solvents and achieves a common (mean) value equal to 0.11 ± 0.02 eV.

The solvent reorganization energy, which describes the motions of the solvent molecules during the charge transfer process may be calculated using the following formula [13]:

$$\lambda_s = \frac{\Delta\vec{\mu}^2}{4\pi hc\varepsilon_0 a^3}\left(\frac{\varepsilon_s - 1}{2\varepsilon_s + 1} - \frac{n^2 - 1}{2n^2 + 1}\right). \tag{1b}$$

Eq. (1) describes experimental findings remarkably well. This can be seen in Fig. 6, which presents a fit of the calculated fluorescence profile to the experimental data for P4 measured in two solvents of different polarity.

According to this pattern, fluorescence of both molecules was analysed to obtain the values of the free enthalpy change (ΔG_{et}) and solvent reorganization energy (λ_s). The results for P4 are presented in Fig. 7.

Similar results were obtained for the compound P3, however systematic reductions of these parameters were observed (the values of ΔG_{et} were smaller (more negative) by 0.15 eV and λ_s by 0.03 eV). For P2 similar analysis yields even smaller values of ΔG_{et} by 0.1 eV and smaller in values of λ_s by 0.05 eV (for solvents of higher polarities). These results indicate that the excited singlet state of cyanoderivative of oxazolo[4,5-*b*]pyridine is lower in energy than that of bromo derivative P3 and unsubstituted compound P2.

It has been found that for compounds P2–P4 the fluorescence quantum yields are close to unity in all investigated

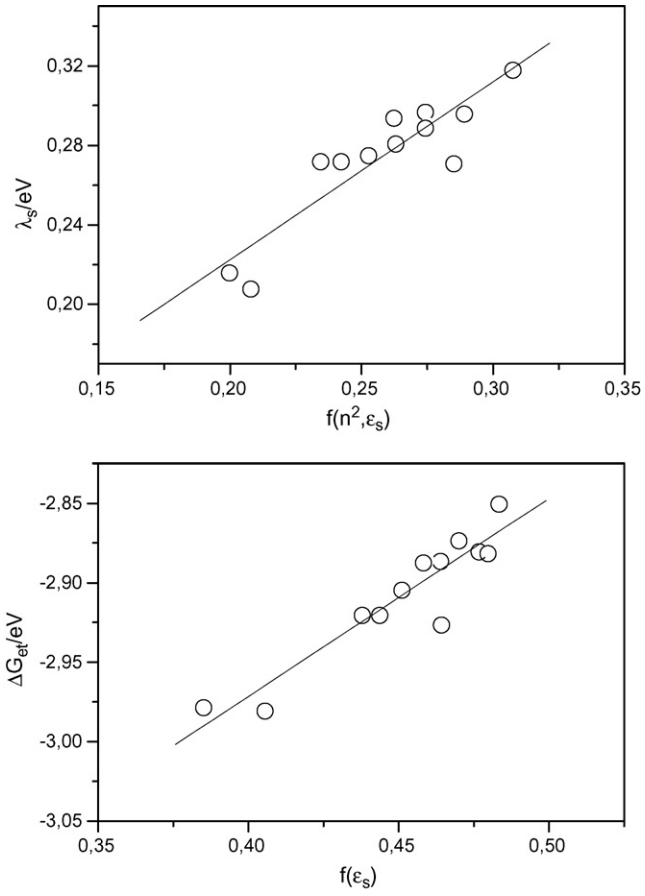

Fig. 7. Dependence of solvent reorganization energy (top) and free enthalpy change (bottom) on solvent polarity functions, as defined by the formulas $f(n^2, \varepsilon_s) = (((\varepsilon_s - 1)/(2\varepsilon_s + 1)) - ((n^2 - 1)/(2n^2 + 1)))$ and $f(\varepsilon_s) = ((\varepsilon_s - 1)/(\varepsilon_s + 1))$ for P4.

aprotic solvents, and the fluorescence lifetimes are rather short (1.4–2 ns for PQ3 and PQ4, respectively, in polar solvents such as acetonitrile), only slightly dependent on the solvent polarity. Noteworthy is the fact that the introduction of bromine into pyridine ring brings only a small decrease of the fluorescence lifetimes and quantum yields. More significant changes in fluorescence properties are observed in aliphatic alcohols, where the lifetimes and fluorescence quantum yields increase with increasing aliphatic chain length of the alcohol. Moreover, the position of the maximum of the first absorption band for P2 is completely insensitive to the polarity of the alcohol. This may indicate formation of complexes of the dye with the proton of the alcohol OH group.

3.1. Acid–base properties of oxazolo[4,5-b]pyridine derivatives

The last results from the previous paragraph inspired us to perform absorptiometric titrations of the all the investigated compounds in protic–aprotic (acetonitrile–water) mixtures. Addition of small amounts of inorganic acids causes a significant change in absorption spectra of these compounds. However, the substances behave differently, i.e. significant difference is observed when we added hydrochloric acid to solutions contain-

ing P1 and P2 or P3 and P4. In the case of P1 the acid addition causes clearly a batochromic shift of the position of the first absorption band. For P2 we observe, beside the batochromic shift of the absorption band, a formation of an absorption band shifted hypsochromically with respect to the first absorption band of the dye in the absence of acid. This case will be discussed at the end of this paragraph in more detail. In the case of the P3 and P4 compounds only a hypsochromic shift was observed.

For the determination of pK_b (the association constant for the reaction $B + H^+ \Leftrightarrow BH^+$, where B denotes the dye) a procedure described in detail in our previous paper has been used [14].

The value of K_b is defined as:

$$K_b = \frac{c_{BH}}{c_{H^+} c_B}. \quad (2)$$

A simple applicoation of the Lambert–Beer relation yields the following equation for K_b

$$F(\text{acid, base}) = \frac{\sum A(\nu)_{BH}}{\sum A(\nu)_B} \frac{\sum \varepsilon(\nu)_B}{\sum \varepsilon(\nu)_{BH}} = K_b c_{H^+}, \quad (3)$$

where the left side of the above equation denotes the ratio of the integrated absorption spectra of the cation BH^+ and that of the neutral dye B multiplied by the ratio of the integrated extinction coefficients of the dye B and its cation BH^+. The above parameters may be easily obtained if the spectra of neutral and cationic forms of the dye are available. If so, then one can easily divide the absorption spectra of the dye in the presence of inorganic acid of concentration c_{H^+} into two components: the cation and the neutral dye. An example is presented below (Fig. 8).

Similar investigations were performed for other dyes (P1, P2 and P4) in acetonitrile–water mixtures at the same water concentrations. The association constants are 13.7, 1470, 361.3 and 94.2 M for the compounds P1, P2 (in the low range of HCl concentration up to 0.01 M), P3, and P4, respectively. This means that association of a proton with the amine nitrogen atom decreases with increasing electron attraction ability of the group introduced in pyridine ring in the 6th position.

A detailed inspection of the acid concentration dependent absorption spectra of P2 shows that the situation is not so clear as in other investigated systems, especially at higher acid concentrations. In the same mixture (7.5 water 2.5 ACN) in the HCl concentration range of 0–1.5 M we observe that upon addition of acid the absorption band located at 380 nm decreases uniformly with simultaneous increase of the bands at 311 nm and 436 nm. However, at higher acid concentration (higher than 0.19 M) the

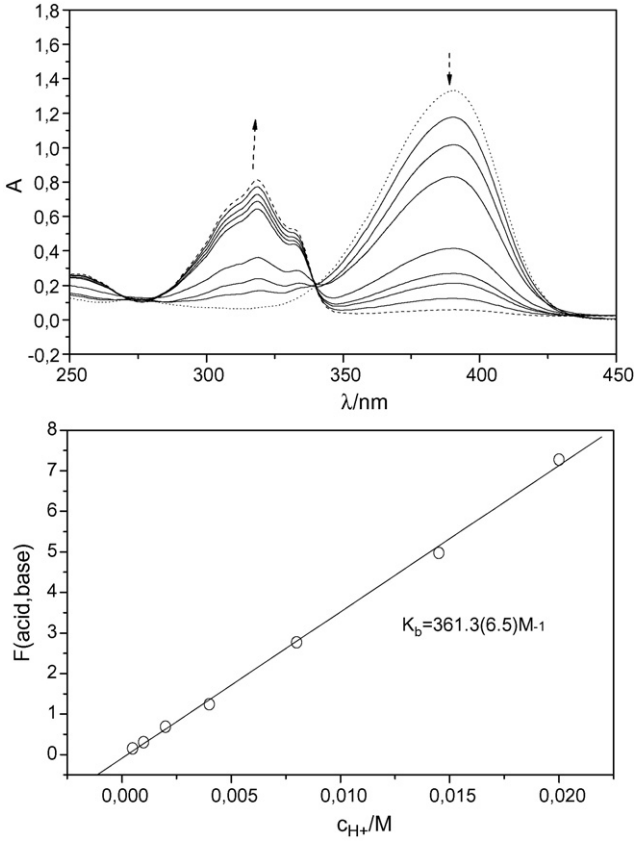

Fig. 8. *Top*: Absorption spectra of P3 in water–acetonitrile mixtures (7.5/2.5 vol./vol.) in the presence of different hydrochloric acid concentrations (in the range of 0–0.05 M). Arrows indicate the decrease and increase of appropriate absorption bands due to the added acid. *Bottom*: Dependence of the relative integrated absorption (see Eq. (3)) on molar concentration of the acid.

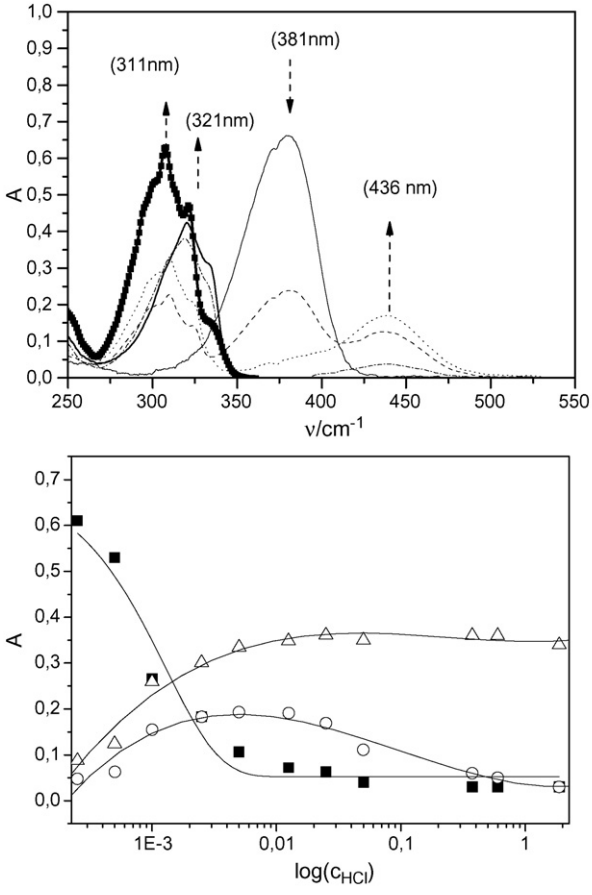

Fig. 9. *Top*: Absorption spectra of P2 in water–ACN mixture in the absence (thin solid) and presence of HCl of concentrations: 2.5×10^{-3} (dashed), 0.025 (dotted), 0.375 (dash-dot), and 1.875 M HCl (bold solid line). Bolded line represents the spectrum of unprotonated P1 in water–acetonitrile mixture. *Bottom*: Concentration profiles of the absorption at 381 (black squares), 436 (open circles) and 311 nm (open triangles), respectively.

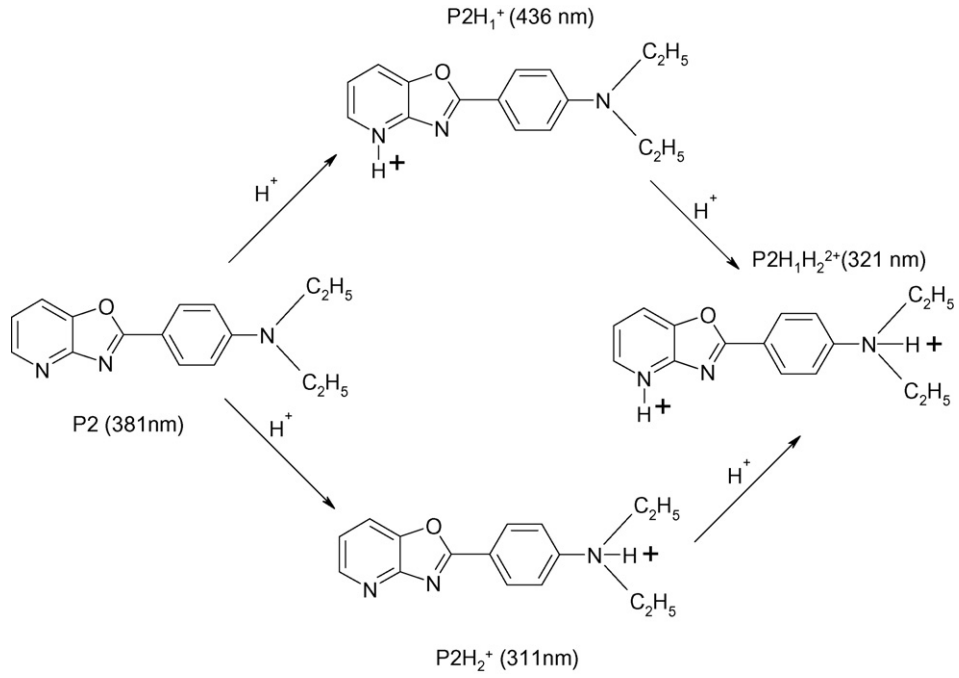

Fig. 10. Protonation of the P2 (2-(4-*N*,*N*-diethylaminophenyl)oxazolo[4,5-*b*]pyridine). In the brackets the positions of the maximum of the absorption bands are indicated.

second band begins to disappear and the first shifts towards lower wavenumbers. Obviously, this result suggests further protonation. Simple comparison of the spectra reveals that the location of the new bands is identical with that of the unprotonated and protonated P1 system.

This is depicted in Fig. 9.

Thus, the complete sequence of the protonation is given in Fig. 10.

We performed also fluorescence titration of all investigated systems. The systems P3 and P4 behave trivially. Addition of the acid causes a decrease of the fluorescence CT band and an appearance of a structured fluorescence (at higher wavenumers) attributed to the protonated species (at the amine nitrogen). Fluorescence of P1 upon addition of the acid is presented in Fig. 11. The structured spectrum of P1 observed in acid-free solution (maximum intensity at 27,930 cm^{-1}) changes at higher acid concentrations to the structureless one, and shifts to higher wavelengths (27,170 cm^{-1}).

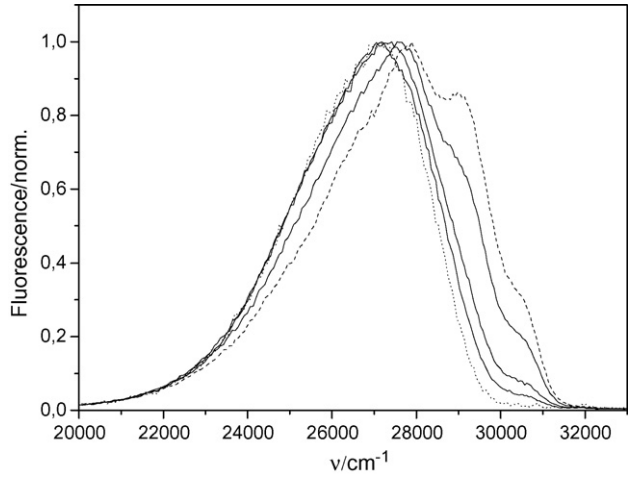

Fig. 11. Fluorescence of P1 in ACN–water mixture (2.5/7.5 vol./vol.) in the absence (dashed line) and in the presence of HCl (excitation: 313 nmHg line). Concentration of acid spans the region 0–0.725 M. The fluorescence at the highest acid concentration is depicted by a dotted line.

Similar feature was observed in the P2 system at medium and high acid concentrations, when monocation $P2H_2^+$ was formed, i.e. in the presence of 0.005M HCl. Again, a slightly structured spectrum is observed (with the maximum of intensity at 27,930 cm^{-1}) which shifts to the red (maximum at 27,170 cm^{-1}) upon further addition of acid. Using the Förster cycle [15] we have determined the pK_b difference for P1 and P2 at medium and higher acid concentration when the $P2H_2^+$ product is formed (see Figs. 8 and 9). From the intersection of normalized fluorescence and absorption bands of the appropriate substances the values of 0–0 transitions for the unprotonated (i.e. P1 and $P2H_2^+$) and the protonated (i.e. P1H and $P2H_1H_2^{2+}$) species were estimated. The differences of pK_b values (i.e. $pK_b^* - pK_b$) are −3.7 and −2.0 for P1 and $P2H_2^+$, respectively. This means that the molecules exhibit a stronger basic character in the excited singlet state.

We performed quantum chemical calculations for the compounds P1, P2 and P4 with special attention to charge distribution in the investigated molecules (in vacuo). For these compounds, the most negative atoms which are accessible to accept protons are: the nitrogen atom in the pyridine ring (No. 1 in Table 1), the N atom located in the oxazole ring (No. 3 in Table 1) and the nitrogen of the amine group in compounds P2–P4 (No. 18 in Table 1).

The results are compiled in Table 1.

Table 1
Atom charges in atomic units (top table) and interatomic distances in Å (bottom table)

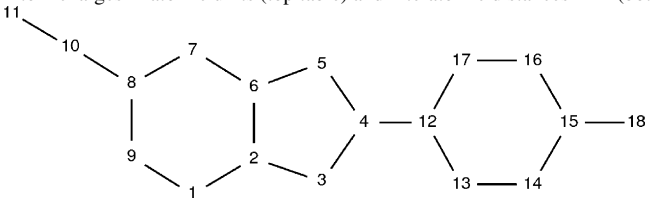

Atom	P1	P2	P3	P4
1 (N)	−0.65	−0.67	−0.73	−0.65
2	0.81	0.82	0.85	0.82
3 (N)	−0.67	−0.70	−0.67	−0.68
4	0.41	0.54	0.44	0.49
5 (O)	−0.31	−0.30	−0.28	−0.28
6	0.10	−0.01	−0.05	0.00
7	−0.11	−0.02	0.13	−0.05
8	−0.41	−0.45	−0.50	−0.32
9	0.26	−0.30	0.51	0.29
10			−0.02 (Br)	0.45 (C)
11				−0.49 (N)
12	0.13	−0.10	0.03	−0.04
13	−0.11	−0.03	−0.09	−0.04
14	−0.13	−0.38	−0.37	−0.39
15	−0.11	0.42	0.49	0.47
16	−0.09	−0.34	−0.35	−0.33
17	−0.19	−0.12	−0.15	−0.14
18		−0.38 (N)	−0.47 (N)	−0.43 (N)

Atom pair	P1	P2	P3	P4
1–2	1.334	1.334	1.333	1.336
2–3	1.389	1.387	1.385	1.379
3–4	1.300	1.304	1.304	1.308
4–5	1.388	1.392	1.395	1.392
5–6	1.368	1.368	1.365	1.365
6–7	1.382	1.381	1.380	1.375
7–8	1.400	1.402	1.400	1.413
8–9	1.408	1.406	1.405	1.416
9–1	1.340	1.342	1.339	1.335
6–2	1.406	1.408	1.407	1.411
8–10			1.903	1.431
10–11				1.165
4–12	1.459	1.449	1.446	1.443
12–13	1.406	1.407	1.408	1.409
13–14	1.393	1.385	1.384	1.384
14–15	1.400	1.422	1.422	1.422
15–18		1.381	1.379	1.377

Numbering according to the scheme at the top. If not specified otherwise, the atoms listed in the table are carbon atoms.

Comparison of the bond lengths in phenyl ring of P1 and P2 molecule shows significant changes upon substitution of the hydrogen atom by the $N(C_2H_5)_2$ group (especially in bonds 13–14 and 14–15). This is consistent with the isomeric structures shown in Fig. 12.

For unsubstitued molecule, only pyridine or oxazole nitrogen atom is a centrum of protonation, whereas for P3 and P4 where the negative charge shifts to the vicinity of the electroaccepting group (Br and CN) only an amine nitrogen atom is susceptible to accept a proton. At this stage of investigation we cannot

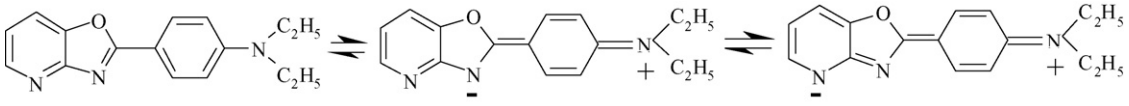

Fig. 12. Resonance structures of P2.

distinguish which atom is protonated in P1 and P2. However, in the case of P3 and P4, where only a hypsochromic shift of the first absorption band is observed, with the formation of the structured spectrum similar to P1 these results show that protonation is mostly at the nitrogen atom of the amine group. The lower association constant for P4 is due to higher electron attractivity of the CN group than bromine. A more pronounced charge transfer character of P4 is visible also in the singlet excited state as, can be observed from the electron transfer parameters obtained from the CT fluorescence analysis.

4. Conclusions

The dyes P2–P4 possess a charge transfer character in the ground and excited states. Very high fluorescence quantum yields of these dyes and rather short fluorescence lifetimes can be explained by very high extinction coefficients of the first absorption band (up to 50,000 $dm^3\,mol^{-1}\,cm^{-1}$). This makes the radiative transition very efficient ($5 \times 10^8\,s^{-1}$), making other possible deactivation processes negligible (i.e. intersystem crossing and internal conversion). Low-temperature phosphorescence (at 77 K) has been observed only for P1 with the lifetime equal to 0.3 s. This is probably responsible for the lack of the internal heavy atom effect, for P3 only a small reduction of the fluorescence parameters (the lifetimes and quantum yields) is observed. For P1 the intersystem crossing seems to play an important role in the deactivation of the singlet excited state (we observed liquid nitrogen phosphorescence and a clear transient absorption attributable for T–T absorption).

The compounds behave like proton indicators. In the case of P2 we can distinguish a complex protonation leading at higher acid concentration to the formation of bication of P2.

Acknowledgements

This work was supported by the State Committee of Scientific Research of Poland (Grants No. 3 T09A 102 18 and 4T09A 109 25). We would like to thank Prof. J. Najbar for diverse help in the course of completion of this project, Dr. P. Kolek for stimulating discussions on quantum chemistry topics, and Dr. K. Jamroży for C^{13} NMR spectra. Quantum chemical calculations were performed on a high-performance SGI Altix 3700 computer in Academic Computer Centre (CYFRONET AGH) in Kraków, Poland.

References

[1] R.L. Clark, A.A. Pessolano, B. Witzel, T. Lanza, T.Y. Shen, C.G. Van Arman, E.A. Risley, J. Med. Chem. 21 (1978) 1158.
[2] T.Y. Shen, R.L. Clark, A.A. Pessolano, B.E. Witzel, T. Lanza, US Patent 4,038,396 (1977);
T.Y. Shen, R.L. Clark, A.A. Pessolano, B.E. Witzel, T. Lanza, Chem. Abst. 87 (1977) 152185.
[3] G. Viscardi, E. Barni, R. Carpignano, J. Heterocyc. Chem. 27 (1990) 1825.
[4] T. Takashi, F. Youneda, Pharm. Bull. 5 (1957) 350.
[5] V. Kalcheva, L. Peshakova, J. Prakt. Chem. 331 (1989) 167.
[6] M.C. Viaud, P. Jamoneau, L. Savelon, G. Guillaimet, Heterocycles 41 (1995) 2799.
[7] S.R. Meech, D. Phillips, J. Photochem. 23 (1983) 193.
[8] M. Mac, A. Danel, K. Kizior, P. Nowak, A. Karocki, B. Tokarczyk, Phys. Chem. Chem. Phys. 5 (2003) 988.
[9] M.J. Frisch, G.W. Trucks, H.B. Schlegel, G.E. Scuseria, M.A. Robb, J.R. Cheeseman, J.A. Montgomery Jr., T. Vreven, K.N. Kudin, J.C. Burant, J.M. Millam, S.S. Iyengar, J. Tomasi, V. Barone, B. Mennucci, M. Cossi, G. Scalmani, N. Rega, G.A. Petersson, H. Nakatsuji, M. Hada, M. Ehara, K. Toyota, R. Fukuda, J. Hasegawa, M. Ishida, T. Nakajima, Y. Honda, O. Kitao, H. Nakai, M. Klene, X. Li, J.E. Knox, H.P. Hratchian, J.B. Cross, V. Bakken, C. Adamo, J. Jaramillo, R. Gomperts, R.E. Stratmann, O. Yazyev, A.J. Austin, R. Cammi, C. Pomelli, J.W. Ochterski, P.Y. Ayala, K. Morokuma, G.A. Voth, P. Salvador, J.J. Dannenberg, V.G. Zakrzewski, S. Dapprich, A.D. Daniels, M.C. Strain, O. Farkas, D.K. Malick, A.D. Rabuck, K. Raghavachari, J.B. Foresman, J.V. Ortiz, Q. Cui, A.G. Baboul, S. Clifford, J. Cioslowski, B.B. Stefanov, G. Liu, A. Liashenko, P. Piskorz, I. Komaromi, R.L. Martin, D.J. Fox, T. Keith, M.A. Al-Laham, C.Y. Peng, A. Nanayakkara, M. Challacombe, P.M.W. Gill, B. Johnson, W. Chen, M.W. Wong, C. Gonzalez, J.A. Pople, Gaussian 03, Revision D.01, Gaussian Inc., Wallingford, CT, 2004.
[10] E. Lippert, Z. Naturforsch 10a (1955) 541;
N. Mataga, Y. Kaifu, M. Koizumi, Bull. Chem. Soc. Jpn. 28 (1955) 690.
[11] R.A. Marcus, J. Phys. Chem. 93 (1989) 3078.
[12] I.R. Gould, R.H. Young, L.J. Mueller, A.C. Albrecht, S. Farid, J. Am. Chem. Soc. 116 (1994) 8188;
I.R. Gould, R.H. Young, R.E. Moody, S. Farid, J. Phys. Chem. 95 (1991) 2068.
[13] J. Herbich, A. Kapturkiewicz, Chem. Phys. 170 (1993) 221.
[14] M. Mac, K. Danel, M. Andrzejak, Polish J. Chem. 80 (2006) 1737.
[15] T. Förster, Z. Elektrochem. 54 (1950) 42.